

RESEARCH ARTICLE

Elevation-dependent response of snow phenology to climate change from a remote sensing perspective: A case survey in the central Tianshan mountains from 2000 to 2019

Huadong Wang¹ | Xueliang Zhang¹  | Pengfeng Xiao¹ | Ka Zhang^{2,3,4} | Senyao Wu¹

¹Jiangsu Provincial Key Laboratory of Geographic Information Science and Technology, Key Laboratory for Land Satellite Remote Sensing Applications of Ministry of Natural Resources, School of Geography and Ocean Science, Nanjing University, Nanjing, Jiangsu, China

²School of Geography, Nanjing Normal University, Nanjing, China

³Key Laboratory of Virtual Geographic Environment (Nanjing Normal University), Ministry of Education, Nanjing, China

⁴Jiangsu Center for Collaborative Innovation in Geographical Information Resource Development and Application, Nanjing, China

Correspondence

Xueliang Zhang, School of Geography and Ocean Science, Nanjing University, Nanjing, 210023, China.
Email: zxl@nju.edu.cn

Funding information

The Special Subject of National Science and Technology Basic Resources Investigation, Grant/Award Number: 2017FY100503; The National Natural Science Foundation of China, Grant/Award Number: 41671344; The Natural Science Foundation of Jiangsu Province of China, Grant/Award Number: BK20201372

Abstract

Alpine snow is an important water resource in arid/semi-arid regions and sensitive to climate change. However, the response of snow phenology to climate change in different elevations remains unclear in mountain areas because of limited observation stations. In this study, the vertical difference of snow phenology and its response to climate change in high mountains are explored by using multi-source remote sensing data from 2000 to 2019, taking the north slope of Central Tianshan Mountains as the study area. The results show that: (1) The temporal changes of snow cover days (SCD), snow cover onset date (SCOD), and snow cover end date (SCED) in different altitudes are various and contribute to the general change trends of the extended SCD, the advanced SCOD, and the advanced SCED from the hydrological year 2000 to 2018; (2) The snow phenology is significantly related to the changed temperature and/or precipitation in most altitudes, except for the SCD and SCOD in high altitudes, where the large temporal changes of temperature and precipitation lead to the complicated correlations in these altitudes; (3) The altitude threshold of 3600 m is identified to separate the relative importance of temperature and precipitation for SCD and SCOD, where the temperature shows a higher importance than precipitation below the altitude threshold, and neither temperature nor precipitation shows constant higher importance above the altitude threshold. As for SCED, the temperature is consistently more important than precipitation in most altitudes.

KEYWORDS

climate change, precipitation, snow phenology, temperature, Tianshan Mountains

1 | INTRODUCTION

Mountainous areas account for approximate one fifth of the earth's land area (Kräuchi et al., 2000). Mountainous snow cover is sensitive to climate change and

plays a vital role in ecosystems and hydrological cycles, as well as providing fresh water for the downstream of mountain rivers (Groisman et al., 1994; Armstrong and Brodzik, 1995; Cayan, 1996; Barry, 2002; Barnett et al., 2005; Viviroli et al., 2011; Wang et al., 2013). In

the context of global warming, snow phenology, which includes the snow cover days (SCD), snow cover onset date (SCOD), and snow cover end date (SCED), is one of the sensitive indicators of climate change and holds great significance in spring water storage and summer flood disasters (Rango, 1997; Ye et al., 2005; Wang and Xie, 2009). In addition, snow phenology characteristics can affect terrestrial ecosystems by changing soil temperature and frozen soil stability (Sinha and Cherkauer, 2008), and thus respond to regional climate changes.

Generally, both ground-measured data and remote sensing data were used to analyse the spatiotemporal changes of snow phenology (Ye, 2001; Wang and Xie, 2009; Chen et al., 2015; Ding et al., 2018). It is noted that due to the scarcity of observation stations in most mountainous areas over the world, it is difficult to adequately quantify the spatiotemporal variability of snow cover in the mountainous regions purely by station data (Woo and Thorne, 2006; Pu et al., 2007). The snow products of the Moderate Resolution Imaging Spectroradiometer (MODIS) have been widely used to describe the temporal and spatial distribution of snow in mountain areas (Hall and Riggs, 2007; Liang et al., 2008; Choubin et al., 2019), showing that the altitude is an indispensable and important factor influencing the temporal and spatial distribution of snow phenology (Redpath et al., 2019). For example, Li et al. (2018) analysed the temporal and spatial distribution and the trend characteristics of the snow cover fraction (SCF) in seven upstream river basins on the Qinghai-Tibet Plateau, finding that the distribution of snow cover is highly dependent on elevations, with a higher SCF and a later onset of snow melt at the higher elevation zones than at the lowers. Sun et al. (2020) used MODIS daily snow products and 1393 ground observation stations to carry out the 2000–2016 Eurasian snow cover spatiotemporal survey, including snow area and snow phenology, finding that the latitude, longitude, and altitude are important factors affecting snow phenology.

In mountain areas, the formation of snow is closely related to the temperature threshold of 0°C. The Intergovernmental Panel on Climate Change (IPCC) reported that the global temperature continues to rise and is expected to rise by 1.5–5.8°C by the end of the 21st century (IPCC et al., 2018). It is generally believed that snow cover is expected to decrease owing to the global warming (Brown and Mote, 2009; Brown et al., 2010; Harpold et al., 2012; Kapnick and Hall, 2012). Studies in the past few decades have shown that SCD, SCF, and snow depth (SD) in the entire

northern hemisphere are decreasing (Brown and Robinson, 2011; Najafi et al., 2016; Hori et al., 2017).

However, the increased precipitation due to rising temperatures (Räisänen, 2008), especially in high latitude and attitude areas will complicate the response of snow cover to global warming. For example, based on the observation stations in the European Alps, it was found that since the late 1980s, SD and SCD have generally decreased, which is related to the increase of the temperature (Scherrer et al., 2004). The ascent rate of temperature in the European Alps is twice the average rate in the northern hemisphere (Auer et al., 2007), and the snow cover changes at high altitudes become more complicated due to the increased precipitation (Hammond et al., 2018). In the Qinghai-Tibet Plateau, the ground station data showed that both the SD and SCD presented an increasing trend from 1961 to 1990, but reversed to a decreasing trend after 1990 (You et al., 2011; Wang et al., 2018). In the Tianshan Mountains of Central Asia, which is an arid and semi-arid region. Aizen et al. (1997) found that the maximum SD and SCD gradually decreased from 1940 to 1991 according to the data from 110 stations. By contrary, Ding et al. (2018) showed that the average and maximum SD increased from 1961 to 2013 in most stations of Tianshan Mountains, Xinjiang, the spatial scope of which is a part of the study area by Aizen et al. (1997).

For mountains with sufficient stations that are continuously distributed in different altitudes, the elevation-dependent response of snow cover changes to temperature and precipitation was explored. Several studies have shown that the correlation between snow cover and temperature in low-altitude areas is enhanced, while in high-altitude areas, the correlation between snow and precipitation is enhanced (Beniston et al., 2003). Scalzitti et al. (2016) studied the correlation between spring snow water equivalent (SWE) and temperature/precipitation in the western mountain areas of the United States, showing that the correlation with temperature decreases linearly with height and the correlation with precipitation increases linearly with height. Besides, the SD of the Swiss Alps (Morán-Tejeda et al., 2013) and the SWE and SCD of the Rocky Mountains (Sospedra-Alfonso et al., 2015) also have the similar law. Based on these studies, it is determined that there is an elevation threshold to determine the relative importance between temperature and precipitation for snow cover (1580–2181 m for mountain areas in the western United States, 1400 ± 200 m for the Swiss Alps, and 1560 ± 120 m for the Rocky Mountains). Below the threshold, the negative correlation with temperature is stronger, and the positive correlation with precipitation is stronger above the threshold. It is noted that the highest altitude involved in

these studies is around 3000 m because of the limitation of observation stations.

However, most mountains, especially those in the developing countries, do not have sufficient observation stations to record the snow information continuously in different altitudes. Accordingly, remote sensing data provides another effective perspective to reveal the elevation-dependent response of snow to climate change. Bi et al. (2015) and Wu et al. (2019) adopted MODIS snow cover data to explore the influence of temperature and precipitation on SCF in different altitudes. Due to the importance of snow phenology in mountain areas and the scarcity of observation stations, the snow phenology and its response to climate change in different altitudes were explored from a remote sensing perspective. The northern slope of Central Tianshan Mountains, Xinjiang, China, is taken as the study area, which is located in the hinterland of the Eurasian Continental, far away from seas comparing with the study areas in the previous related studies, for example, Alps, Rocky Mountains. In addition, the highest elevation of our study area is higher than 5000 m, which is beneficial from the remote sensing data without the limitation of station distribution.

The main objectives of this study are: (1) to validate the feasibility of exploring elevation-dependent response of snow phenology to climate change from a remote sensing perspective; (2) to reveal the distribution characteristics of snow phenology and its temporal variations at different altitudes; and (3) to understand the vertical difference of the response of snow phenology to temperature and precipitation.

2 | STUDY AREA AND DATA

2.1 | Study area

The study area is located in the northern slope of Central Tianshan Mountains in Xinjiang, Northwest China (43°1'20"N–44°26'51"N, 83°24'27"E–87°42'19"E), with an area of approximately 63,275 km² (Figure 1). The altitude ranges from 421 to 5012 m from north to south, and the characteristics of vertical zonality are considerably clear (Hu, 2004; Feng et al., 2018). It is the first mountain barrier for Arctic water vapour to enter Central Asia and is an ideal research area for studying climate change in northern Central Asia (Aizen et al., 1997). The region is located in the mid-latitude westerly zone with a typical continental arid and semi-arid climate. In addition, since the precipitation is limited, the mountainous snow in this region serves as an important water source for the oasis in the lower reaches of mountain rivers, especially in the

spring with large agricultural water consumption (Hu, 2004; Feng et al., 2018). Hence, understanding the snow phenology as well as its impactors is of great significance to the local climate, water resources, and ecological environment.

2.2 | Data

Due to the scarcity of observation stations, the remote sensing data are adopted in this study to provide the cell-wise information of snow cover, temperature, and precipitation. To characterize the snow phenology, the MODIS daily snow cover products MOD10A1 and MYD10A1 (V6) from 2000 to 2019 are used. The daily land surface temperature (LST) product MOD11A1 and the China meteorological forcing dataset (CMFD) are used to provide the temperature and precipitation information, respectively. It is noted the study period of this study is constrained by CMFD because it only provides data until 2018. The daily snow depth in nine meteorological stations and daily temperature and precipitation in three meteorological stations are used to validate the accuracy of these products. In addition, 63 Landsat Operational Land Imager (OLI) images, which cover all the available Landsat OLI images with cloud cover <10% in the study area from the hydrological year 2018 to 2019, are also used for validating snow cover data in high altitude areas because most of the stations are located in low altitude areas. The Shuttle Radar Topography Mission (SRTM) digital elevation model (DEM) is adopted to divide the study area into 45 altitude belts with an interval of 100 m, where the region from 4800 to 5012 m is viewed as one belt because of the small number of cells. Table 1 presents the detailed information of each data.

The daily snow cover products MOD10A1 and MYD10A1 are produced by the snow mapping (SNOMAP) algorithm, which have been globally validated with high accuracy and temporal continuity, with a spatial resolution of up to 500 m (Hall et al., 1995, 2002; Hall and Riggs, 2007; Parajka and Blöschl, 2008; Huang et al., 2011; Dietz et al., 2012). The mean LST error of MOD11A1 is within ± 0.6 K in 10 validate datasets (Wan, 2014). CMFD is the high spatial-temporal resolution gridded near-surface meteorological dataset in China, which was made through fusion of remote sensing products, reanalysis datasets and in-situ station data (He et al., 2020). We use daily temperature and precipitation in three stations to verify the accuracy of the LST and CMFD in our study area, and the results are shown in Figure 2. The R^2 between the LST and station temperature is 0.888, and that of precipitation is 0.337.

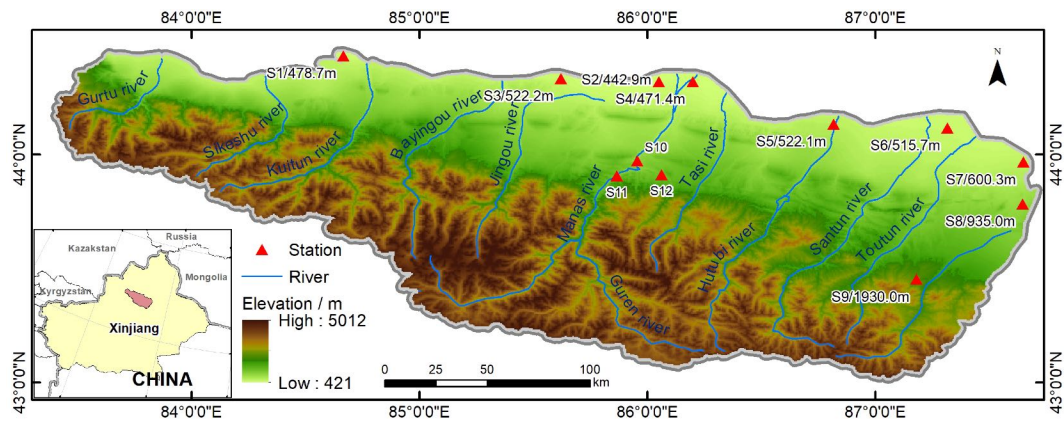


FIGURE 1 Location of the northern slope of central Tianshan Mountains in Xinjiang, Northwest China, as well as the elevation and the location of meteorological stations in this region. S1–S9 record snow depth and S10–S12 record temperature and precipitation [Colour figure can be viewed at wileyonlinelibrary.com]

TABLE 1 Details of the data used in this study

Type	Name	Spatial resolution	Temporal resolution	Time range
Snow cover	MOD10A1/MYD10A1	500 m	1 day	1 September 2000 to 31 August 2019
Temperature	MOD11A1	1,000 m	1 day	1 September 2000 to 31 August 2018
Precipitation	China meteorological forcing dataset	0.1°	1 day	1 September 2000 to 31 August 2018
Elevation	DEM	90 m	–	–
Temperature & precipitation	Meteorological station	–	1 day	1 January 2003 to 30 September 2011
Snow depth	Meteorological station	–	1 day	1 September 2002 to 31 May 2019
–	Landsat OLI	30 m	16 days	1 September 2018 to 31 August 2019

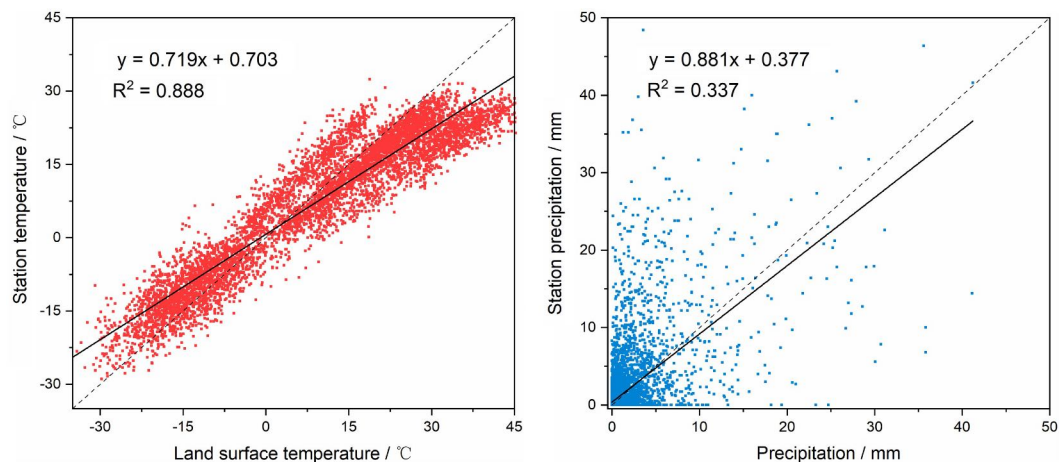


FIGURE 2 Scatterplots of meteorological station records against MOD11A1 and CMFD precipitation [Colour figure can be viewed at wileyonlinelibrary.com]

3 | METHOD

3.1 | Snow phenology extraction

The snow phenology features of SCD, SCOD, and SCED are calculated by the daily snow cover products MOD10A1 and MYD10A1. Since the heavy cloud contamination of the daily products would seriously affect the accuracy of the extracted snow phenology, the cloud removal method proposed by Gafurov and Bárdossy (2009) is firstly applied to obtain cloud-free products. This method is widely used for MODIS daily snow products because of its good cloud removal effect (Tong et al., 2009; Xie et al., 2009).

The cloud-free daily snow cover data are validated by both Landsat OLI images and meteorological station data. The SNOMAP algorithm is used to generate the snow cover map by Landsat OLI images (Hall et al., 1995). The NDSI threshold is set as 0.4 for both Landsat OLI images and MODIS snow cover products. Table 2 shows the confusion matrix by comparing the

cloud-removed MODIS daily products with the Landsat OLI images and the daily meteorological station observations, where the station observation with snow depth greater than or equal to 3 cm is viewed as snow (Yang et al., 2015). The overall accuracy validated by 2457 station observations is 80.79%, where the main error comes from the omission error because most of the stations are located near urban area. The overall accuracy validated by Landsat OLI images is 82.67%, where the main error comes from the commission error because of the complex terrain in high mountains. The snow cover maps from MODIS and Landsat OLI are shown in Figure 3 to visually show the consistency between them.

The SCD refers to the cumulative number of snow cover days observed in a hydrological year (1 September to 31 August of the following year) (Ke et al., 2016; Notarnicola, 2020). We synthesized the cloud-removal daily snow cover products into 8 days snow cover data because of the omission errors validated by station observations as shown in Table 2. The synthesizing method is

MODIS	Landsat OLI			Meteorological stations		
	Snow	Land	Total	Snow	Land	Total
Snow	268,479	426,838	695,317	661	12	673
Land	70,996	1,669,692	1,740,688	460	1324	1784
Subtotal	339,475	2,096,530	2,436,005	1121	1336	2457
Overall accuracy	82.67%			80.79%		

TABLE 2 Accuracies of cloud-free MODIS snow cover data validated by meteorological station observations and Landsat OLI images

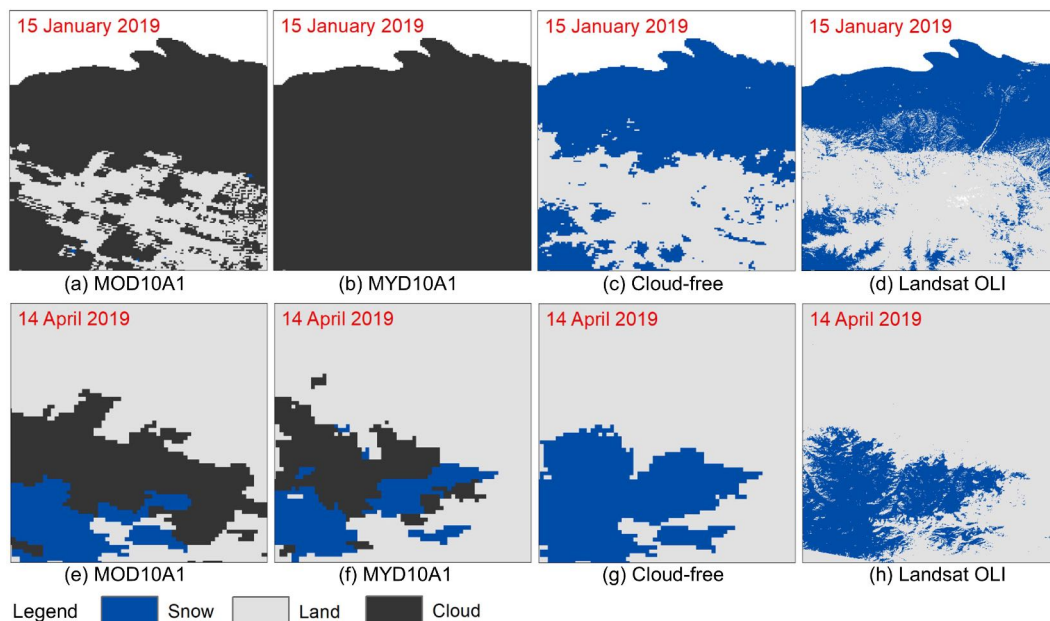


FIGURE 3 Snow cover maps retrieved from MOD10A1, MYD10A1, cloud-free snow cover data, and Landsat OLI image [Colour figure can be viewed at wileyonlinelibrary.com]

same as that of producing the MODIS 8 days snow cover product MOD10A2, in which a synthesized cell is identified as snow if there is snow in a cell for any day within 8 days. SCD is then extracted from the synthesized 8 days snow cover data. It is noted that we do not directly use the 8 days product MOD10A2 to calculate SCD because the synthesized data from cloud-removed daily products could achieve higher SCD accuracy. The calculation method of SCD is as follows:

$$SCD = 8 \sum_{i=1}^n (S_i), \quad (1)$$

where S_i represents a pixel value with 1 indicating snow and 0 non-snow in the synthesized data, and n represents the number of the synthesized data within a hydrological year.

The SCOD and SCED are defined as the first day and the end day of the continuous snow cover days observed during a hydrological year, respectively (McKay and Thompson, 1968; Gao et al., 2011; Chen et al., 2015; Sun et al., 2020). It is noted that using the continuous multi-day method can reduce the impact of short-term snow cover on SCOD and SCED. Specifically, the continuous 5-days method is adopted to extract SCOD and SCED (Choi et al., 2010; Peng et al., 2013; Chen et al., 2015; Sun et al., 2020). SCOD and SCED are extracted from the cloud-free daily snow cover products, and the calculation method is as follows:

$$SCOD = \min\{t\} \mid \left\{ t \in [0, m-4] \text{ and } \sum_{k=0}^4 S_{t+k} = 5 \right\}, \quad (2)$$

$$SCED = \max\{t\} + 4 \mid \left\{ t \in [0, m-4] \text{ and } \sum_{k=0}^4 S_{t+k} = 5 \right\}, \quad (3)$$

where t indicates a date, m is the number of dates in a hydrological year, and S_t represents the value of a pixel with 1 indicating snow and 0 non-snow. Since the cloud is not totally removed, the cloud pixel is viewed as snow for the calculation if there is snow within 5 days, which could reduce the negative influence of cloud pixels but brings the additional risk of obtaining advanced SCOD and delayed SCED.

3.2 | Temporal change trend analysis

The unary linear regression model is adopted for analysing the temporal change trend of snow phenology,

temperature, and precipitation, where the slope of the regression line quantifies the temporal change rate (Equation [4]).

$$Slope = \frac{n \times \sum_{i=1}^n i \times X_i - \sum_{i=1}^n i \sum_{i=1}^n X_i}{n \times \sum_{i=1}^n i^2 - \left(\sum_{i=1}^n i \right)^2}, \quad (4)$$

where i is the serial number from 1 to 19 for the hydrological years from 2000 to 2018, and X_i is the pixel value in the i th year, representing the snow phenology, temperature, or precipitation. The greater the absolute value of slope, the faster the rate of change is indicated.

3.3 | Mann-Kendall test

We use the nonparametric Mann-Kendall analysis to test the trend significance (Hamed and Rao, 1998). It does not require that the snow phenology data obey a normal distribution, nor does it require that the change trend is linear. The calculation formula is as follows:

$$S = \sum_{i=1}^{n-1} \sum_{j=i+1}^n \text{sgn}(x_j - x_i), \quad \text{sgn}(x_j - x_i) = \begin{cases} 1, & x_j > x_i \\ 0, & x_j = x_i \\ -1, & x_j < x_i \end{cases} \quad (5)$$

$$Z = \begin{cases} \frac{S-1}{\sqrt{\text{Var}(S)}}, & S > 0 \\ 0, & S = 0 \\ \frac{S+1}{\sqrt{\text{Var}(S)}}, & S < 0 \end{cases}, \quad \text{Var}(S) = \frac{n(n-1)(2n+5)}{18} \quad (6)$$

where x_j and x_i is the pixel value, n represents the number of the years. At a given significance level α , when $|Z| > |Z_{1-\alpha/2}|$, it means that the temporal change trend is significant.

3.4 | Correlation analysis

The correlation between the snow phenology and the meteorological factors is calculated by the Pearson correlation method. The Pearson correlation coefficient r is defined as the product of the covariance of the two variables x and y divided by their standard deviation as follows:

$$r = \frac{n(\sum xy) - (\sum x)(\sum y)}{\sqrt{[n\sum x^2 - (\sum x)^2][n\sum y^2 - (\sum y)^2]}}, \quad (7)$$

where the variable x represents snow phenology, y represents precipitation or temperature, and n is the number of variables involved in the operation, which equals to 18 in this study. The correlation analysis is performed for each altitude belt to show the elevation-dependent response of snow phenology to climate change. The correlation coefficient r is tested at the 95% significance level.

Considering the continuous influence of temperature and precipitation on snow phenology, the accumulated precipitation and average temperature in a certain period from SCOD to SCED are calculated for correlation analysis with the time step of 1 month. However, since we are not sure which months are sensitive for snow phenology, the correlation coefficients are compared among different periods, and the largest r value is chosen as the coefficient and the corresponding period is viewed as the sensitive period for snow phenology.

4 | RESULTS

4.1 | Validation of the extracted snow phenology

The snow phenology (SCD/SCOD/SCED) extracted from cloud-free MODIS snow cover data are evaluated by the observed snow depth of nine meteorological stations from 2002 to 2018. As shown in Figure 4, the average SCD extracted by MODIS is roughly consistent with the SCD extracted by the meteorological stations and the average difference between them is approximately 10 days. It is noted that the average difference would

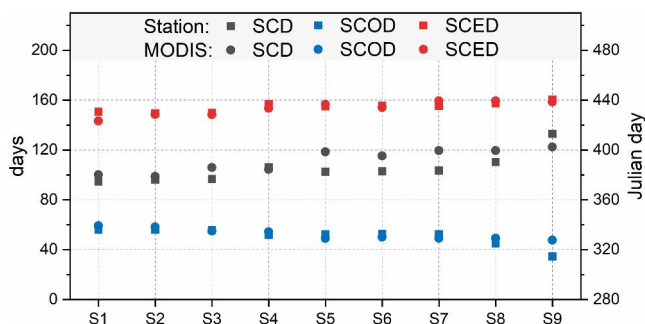


FIGURE 4 Comparison of snow phenology between MODIS and in-situ observations at nine meteorological stations, where the SCD refers to the left y-axis, and the SCOD and SCED refer to the right y-axis [Colour figure can be viewed at wileyonlinelibrary.com]

increase to 18 days if directly using the MOD10A2 for calculating SCD. In addition, the average difference would be 29 days if directly using the daily cloud-free MODIS snow cover data for calculating SCD.

As for the SCOD and SCED, the data extracted by the daily cloud-free MODIS snow cover data and the meteorological stations are also consistent with the average difference smaller than 4 days. In most cases, the SCOD extracted by MODIS are later than that of the meteorological stations and SCED are earlier, which is mainly because the omission error and the scale and time difference between station and remote sensing data. Since the snow is sparsely distributed at the beginning of snow accumulated period and in the end of the snow melting period, the MODIS pixel may not be recognized as snow because of the small snow fraction while at the same time it is still recorded as snow by the station, which results in the later SCOD and the earlier SCED by MODIS than that by meteorological stations.

4.2 | Temporal change of snow phenology

The temporal changes of snow phenology, temperature, and precipitation in the whole region as well as in each altitude belt from the hydrological year 2000 to 2018 are calculated and presented in Figure 5.

As shown in Figure 5a, the average SCD in these years is 160 days with the longest SCD of 177 days in 2010 and the shortest SCD of 139 days in 2001. SCD shows an overall growing trend at a growth rate of $0.567 \text{ day}\cdot\text{a}^{-1}$. The growing trend of SCD in the whole region is not significant because the SCD change direction in the middle altitudes is opposite to that in the low altitudes, and the SCD in the high altitudes remains almost unchanged, as shown in Figure 5f. The SCD in the altitude belts between 2600 and 3500 m are significantly extended (approximately $1.2 \text{ day}\cdot\text{a}^{-1}$).

The average SCOD is on 10 November with fluctuation smaller than 10 days, as shown in Figure 5b. SCOD is advanced at a rate of $0.429 \text{ day}\cdot\text{a}^{-1}$, which is because the SCOD are advanced in most altitudes, especially in the middle altitude belts between 1500 and 1900 m with a significant changing rate of $-0.7 \text{ day}\cdot\text{a}^{-1}$, as shown in Figure 5g.

The average SCED is on 14 April with small fluctuation smaller than 10 days, as shown in Figure 5c. The SCED advances at a rate of $0.319 \text{ day}\cdot\text{a}^{-1}$, and the change in each altitude belt is not significant. In addition, the SCED in the low and high altitudes are almost unchanged, as shown in Figure 5h.

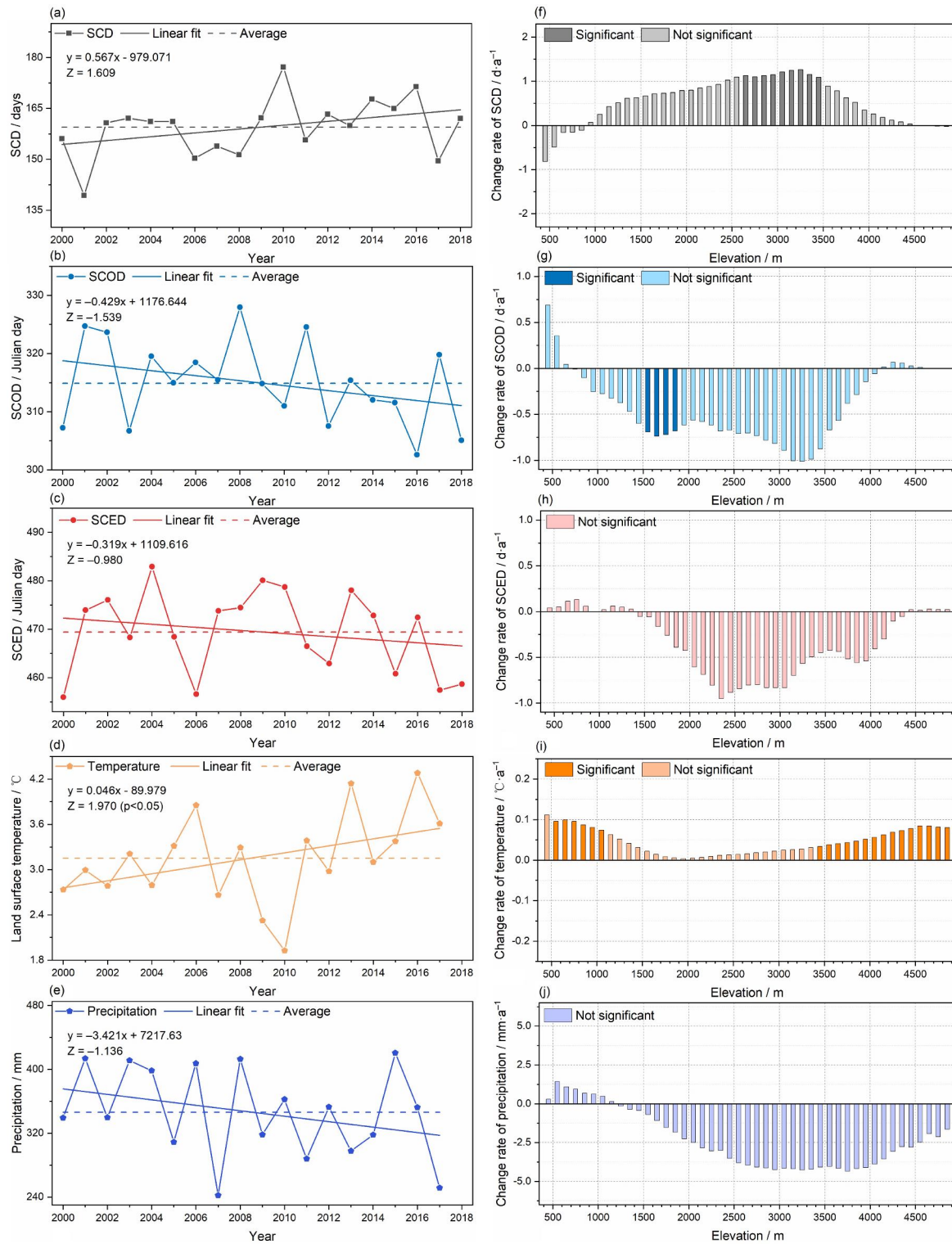


FIGURE 5 Temporal change of the snow phenology (SCD/SCOD/SCED), temperature, and precipitation indicated in the whole region (a–e) and each altitude belt (f–j) from the hydrological year 2000 to 2018 [Colour figure can be viewed at wileyonlinelibrary.com]

The extended SCD, together with the advanced SCOD/SCED may be related to the changed temperature and precipitation. The temperature in the whole region significantly increases ($0.046^{\circ}\text{C}\cdot\text{a}^{-1}$) and the

precipitation slightly decreases ($-3.421\text{ mm}\cdot\text{a}^{-1}$), as shown in Figure 5d,e, respectively. This is because the temperature increases in all altitudes, and especially at low and high elevation, the change is significant, as

shown in Figure 5i. The precipitation increases below 1200 m and decreases above it, but the changes of precipitation in each altitude are all not significant, as shown in Figure 5j.

Usually, the snow phenology indicated by meteorological station observation datasets, such as those by Ke et al. (2016), Ma et al. (2020), and Peng et al. (2013), shows that the SCD is shortened, the SCOD is delayed

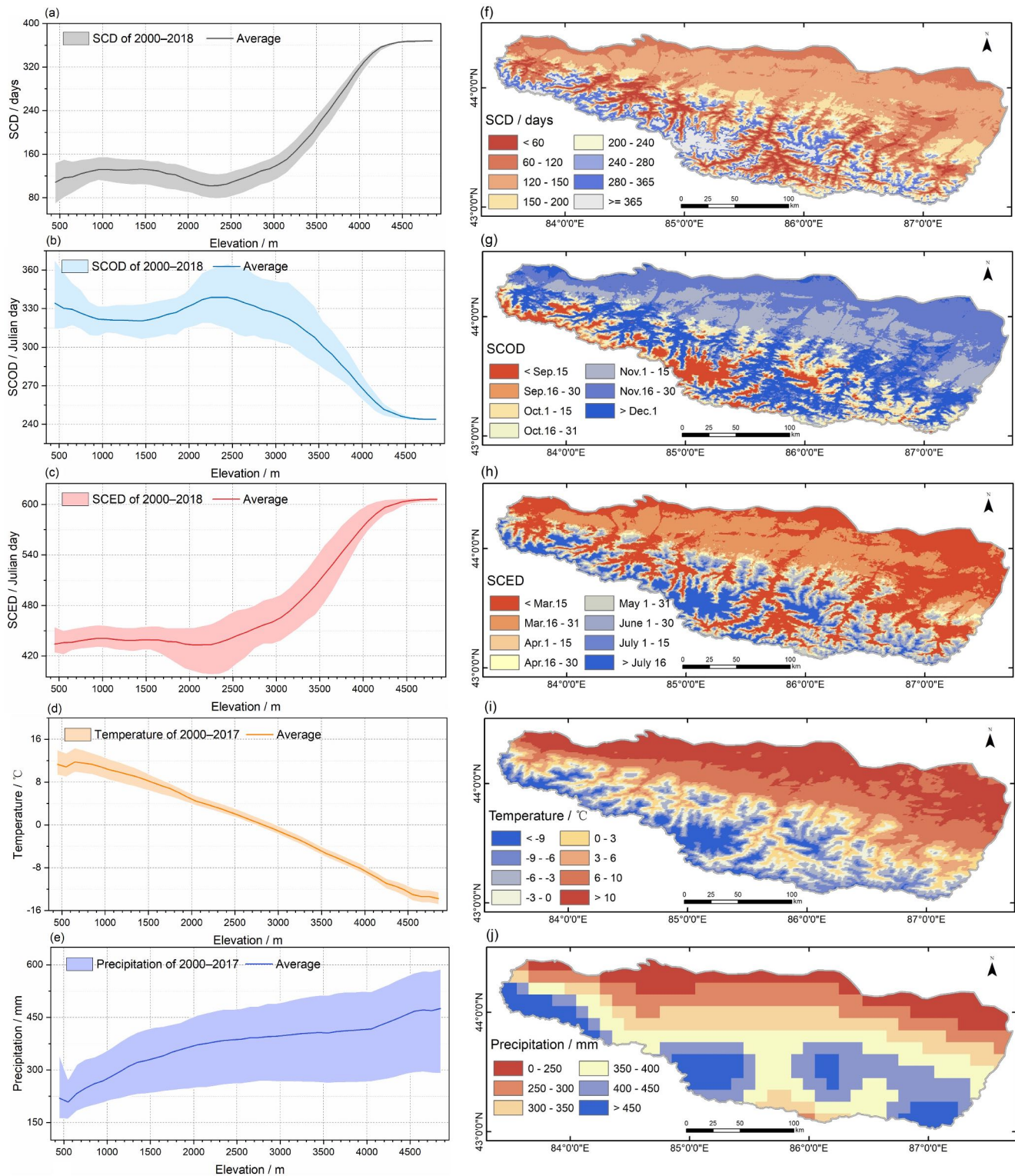


FIGURE 6 Vertical change (a–e) and specialisation (f–j) of the multi-year average of snow phenology (SCD/SCOD/SCED), temperature, and precipitation from the hydrological year 2000 to 2018 [Colour figure can be viewed at wileyonlinelibrary.com]

and the SCED is advanced in Northern Hemisphere. It is noted that most of the meteorological stations are located at relatively low elevations. As shown in Figure 5f,g,h, we could find the decreased SCD, delayed SCOD and slightly delayed SCED in the low elevations by remote sensing data. Hence, the opposite change trend of SCD and SCOD in the whole study area may attribute to the snow cover change in the middle and high elevations. Similarly, Tang et al. (2017) found a similar change in Tianshan Mountains by using the MODIS snow cover products from 2001 to 2015, with an SCD increase of 9.36% and 7.47% in the Northern and Western Tianshan Mountains, respectively. In addition, we also need to consider the different time periods. For example, the above three previous studies were from 1952 to 2010 (Ke

et al., 2016), 1970 to 2014 (Ma et al., 2020), and 1980 to 2006 (Peng et al., 2013), while ours is from 2000 to 2019.

4.3 | Vertical distribution of snow phenology

The temperature and precipitation are changed with the altitude, which result in the various snow phenology at different altitudes. To reflect the vertical differences, we calculated the multi-year average values of snow phenology, temperature, and precipitation in each altitude belt, and the changing curves with altitude are shown in Figure 6a–e. To further illustrate the spatial distribution, the multi-year average snow phenology,

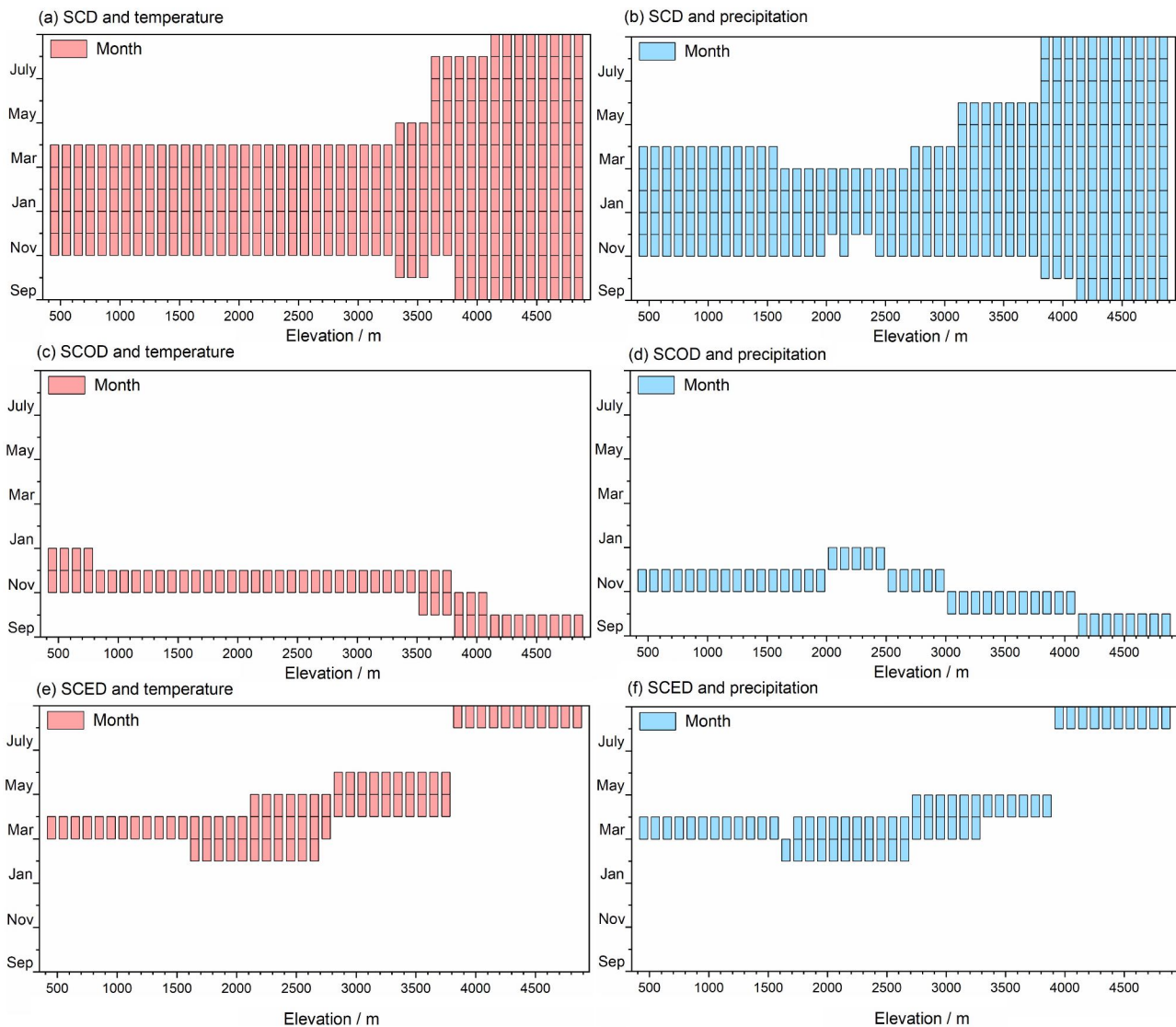


FIGURE 7 Sensitive periods for the response of snow phenology to temperature/precipitation in each altitude belt, where the sensitive period is determined as that with the maximum correlation coefficient between snow phenology and temperature/precipitation. (a), (c), and (e) are the sensitive periods for SCD, SCOD, and SCED to temperature, and (b), (d), and (f) are the sensitive periods for SCD, SCOD, and SCED to precipitation [Colour figure can be viewed at [wileyonlinelibrary.com](https://onlinelibrary.wiley.com)]

temperature, and precipitation are mapped and shown in Figure 6f–j.

Figure 6a shows that the SCD continues to increase from 108 to 132 days at a growth rate of $2.4 \text{ days} \cdot (100 \text{ m})^{-1}$ below 1000 m, and almost unchanged between 1000 and 1500 m. There is a small valley in the SCD curve between 1500 and 2500 m, indicating that the SCD decreases compared with that in relatively lower altitudes. This is mainly resulted from the decreased SCD in the mountain valleys as indicated by Figure 6f, which may be caused by the higher temperature of the valleys than the surrounding area, as shown in Figure 6i. The SCD increases quickly at the rate of $13.2 \text{ days} \cdot (100 \text{ m})^{-1}$ between 2600 and 4500 m, and then becomes stable above 4500 m because of the permanent snow, which should be related to the glaciers (Zhu et al., 2014), as shown in Figure 6f. The cross-year fluctuations of SCD decrease from 76 to 2 days with the increased altitude.

The SCOD generally tends to advance from Julian day 338 (late December) to 243 (early September) with the increased altitude but presents different advancing rates at different altitudes, as shown in Figure 6b. The advancing rate is only $1.4 \text{ day} \cdot (100 \text{ m})^{-1}$ below 1500 m. It has a small peak between 1500 and 2500 m, which may be also caused by the relatively high temperature in the mountain valleys. Then the SCOD advances at the rate of $4.8 \text{ days} \cdot (100 \text{ m})^{-1}$ and finally achieves stable above 4500 m. As the altitude increases, the temporal fluctuations of SCOD tends to increase at first, achieves the maximum of 54 d around 2700 m, and then turns to decrease until 4500 m.

The vertical change of SCED is opposite to that of SCOD. As shown in Figure 6c, the SCED is gradually delayed from Julian day 433 (early March) to 608 (late August) as the altitude increases. The delay of SCED with altitude is relatively slow at the rate of $1.6 \text{ d} \cdot (100 \text{ m})^{-1}$ below 1000 m, and changes to advance between 1500 and 2500 m like SCD and SCOD. After the altitude of 2500 m, the delay rate change to be quick at the rate of $8 \text{ days} \cdot (100 \text{ m})^{-1}$ until 4500 m, and then the SCED also becomes stable. The temporal fluctuations of SCED increase first and then decrease from 69 to 4 days.

As the altitude increases, the temperature continues to decrease as shown in Figure 6d. It is noted that the vertical change rate of temperature for the entire altitude is $0.6^\circ\text{C} \cdot (100 \text{ m})^{-1}$, and the average temperature is below 0°C above 2700 m. The precipitation gradually increases with the altitude until 4000 m at the rate of $2.3 \text{ mm} \cdot (100 \text{ m})^{-1}$, and turns to increase quickly above 4000 m at the rate of $4.4 \text{ mm} \cdot (100 \text{ m})^{-1}$, as shown in Figure 6e. The temporal fluctuations of the temperature tend to decrease with the increased altitude, while those of the precipitation tend to increase.

4.4 | Vertical difference of the response of snow phenology to climate change

Since the snow phenology and temperature/precipitation change with altitude, the correlation analysis between snow phenology and temperature/precipitation is performed at each elevation belt to reveal the vertical difference of the response of snow phenology to climate change. As described in Subsection 3.3, the sensitive periods for SCD/SCOD/SCED in each altitude belt are determined as the continuous months with the maximum correlation coefficient to temperature/precipitation, as shown in Figure 7. Since the SCOD advances and the SCED delays with altitude, the sensitive period for SCD extends from November–March to September–August with the increased altitude, and the sensitive periods for

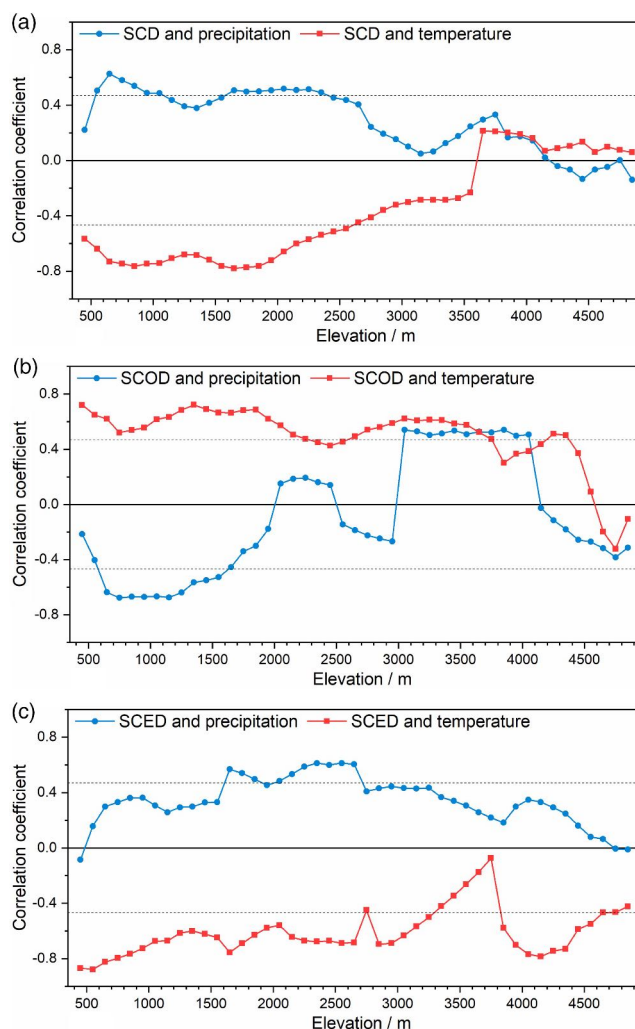


FIGURE 8 Correlation coefficients between the snow phenology of SCD (a), SCOD (b), SCED (c) and temperature/precipitation in each altitude belt, where the dashed line indicates the correlation coefficient at the 95% significance level [Colour figure can be viewed at wileyonlinelibrary.com]

SCOD and SCED are various in different altitudes because they are high dependent on the date of SCOD and SCED, respectively. As for the SCOD, the sensitive period to temperature/precipitation varies from September to December as the altitude decreases, and the most period lengths are only 1 month, as shown in Figure 7c,d. In addition, the sensitive periods are similar between temperature and precipitation in most altitudes. As for the SCED, the length of the sensitive period for SCED and temperature/precipitation ranges from 1 month to 3 months in different altitudes, and the length tends to be longer in the middle altitudes, as shown in Figure 7e,f.

Constrained by the sensitive periods, the correlation coefficient values between snow phenology and temperature/precipitation in each altitude are calculated and presented in Figure 8. In addition, to further illustrate

the influence of the changed temperature/precipitation on snow phenology, the temporal change rates of temperature/precipitation in the different sensitive periods at each altitude belt are calculated and shown in Figure 9.

In Figure 8a, the SCD is negatively correlated with temperature below 3600 m, while it is positively correlated with precipitation below 4100 m. The negative correlation between SCD and temperature indicates that the lower temperature leads to the longer SCD, and the positive correlation between SCD and precipitation indicates that the more precipitation leads to the longer SCD. The correlations between SCD and temperature/precipitation tend to decrease along with the increased altitude, which are significant below 2600 m and not significant above that. The nonsignificant correlation from 2600 to 3500 m is because the SCD changes significantly in these altitudes but at the same time the temperature/precipitation changes

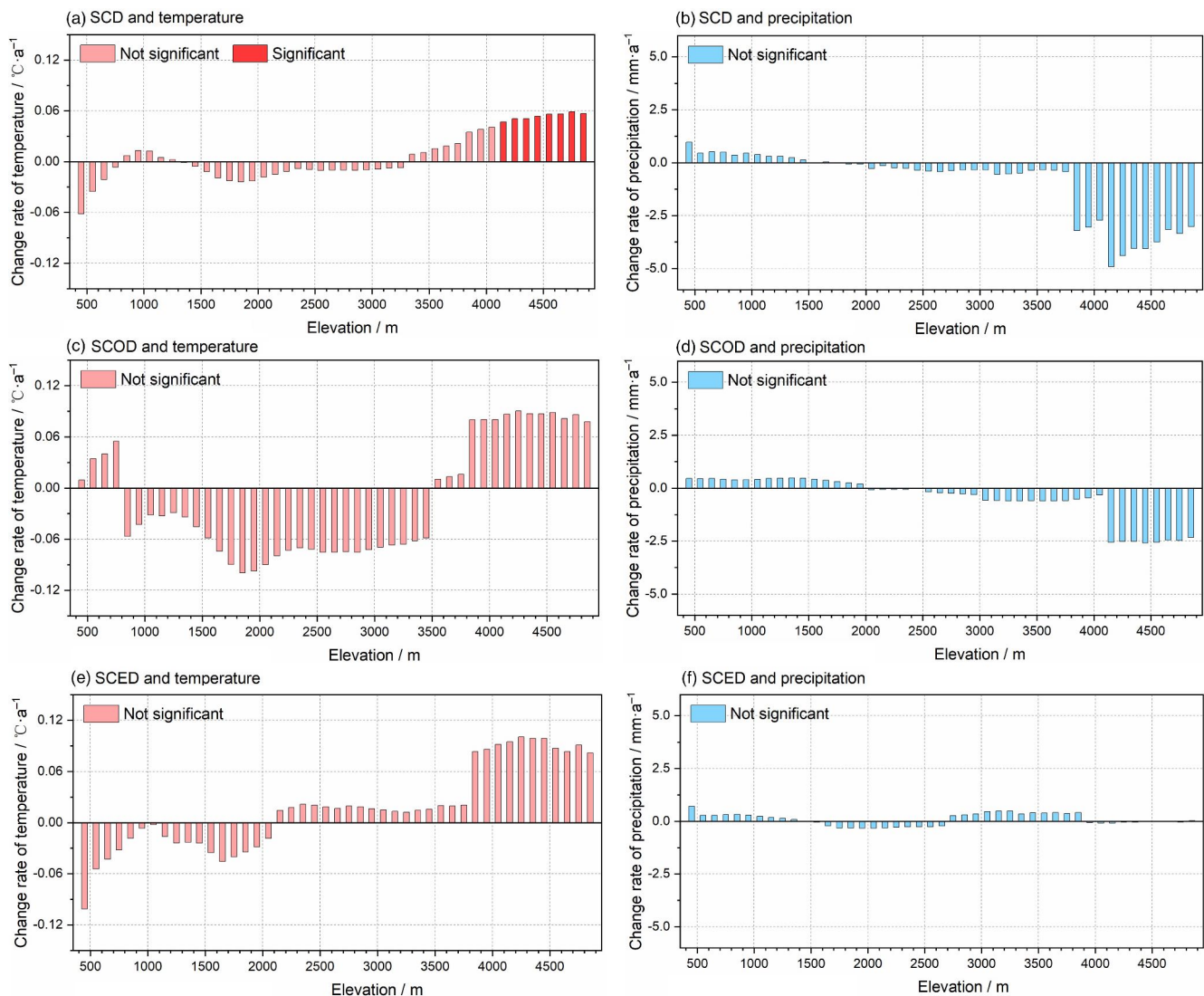


FIGURE 9 Temporal change of the temperature (a, c, e) and precipitation (b, d, f) in the sensitive periods to snow phenology (SCD, SCOD, and SCED from top to bottom) from the hydrological year 2000 to 2017 [Colour figure can be viewed at wileyonlinelibrary.com]

are not significant, as shown in Figures 5f and 9a,b. In high altitudes, the correlations turn to be abnormally positive for SCD and temperature, and negative for SCD and precipitation, both of which are not significant. The abnormal correlations may be caused by the slightly extended SCD together with the significant increase of temperature and the large decrease of precipitation in these altitudes.

As shown in Figure 8b, the correlations between SCOD and temperature are positive in most altitudes except for those above 4500 m, indicating that the lower temperature contributes to advanced SCOD. It is noted that most of the positive correlations below 3500 m are significant, which may be caused by the decreased (increased) temperature coincide with the advanced (delayed) SCOD in these altitudes, as shown in Figures 5g and 9e. The correlations decrease to be non-significant and even to be abnormally negative above 3500 m, which is because the temperature increases apparently while SCOD only changes slightly in these altitudes. The correlations between SCOD and precipitation are negative in most altitudes and turns to be abnormally positive in altitudes 2000–2500 m and 3000–4100 m. The abnormally positive correlation in 2000–2500 m may be caused by the mountain valleys, where the temperature is higher than the surrounding area and prevents to new fallen snow to be accumulated. The abnormally positive correlation in 3000–4100 m may be caused by the coincidence of the advanced SCOD and the decreased precipitation in these altitudes.

Figure 8c shows that the correlations between SCED and temperature are all negative, indicating that the increased temperature contributes to the advanced SCED. In most cases, the negative correlations are tested to be significant. On the contrary, the correlations between SCED and precipitation are almost all positive, indicating that the decreased precipitation contributes to the advanced SCED. The positive correlations are only significant in the middle altitudes from 1600 to 2800 m.

5 | DISCUSSION

5.1 | What is the relation between the changed SCD and the changed SCOD/SCED in different altitudes?

We already know that the general change trend of SCD, SCOD, and SCED in the study area by Figure 5, where the extended SCD corresponds to the advanced SCOD and the slightly advanced SCED. However, since the change rate and the change direction of SCD, SCOD, and SCED are various in different altitudes, we try to explore whether the change of SCD in each altitude is mainly related to SCOD or SCED or both of them.

In the low altitudes below 900 m, the SCD is shortened as shown in Figure 5f. Correspondingly, the SCED is delayed in these altitudes as shown in Figure 5h that should lead to longer SCD. However, as the SCOD is advanced (Figure 5g), the SCD is correspondingly shortened. In this case, the shortened SCD could be mainly related to the SCOD in these altitudes.

In the altitudes between 900 and 4500 m, the SCD is extended. We can see that the SCD change rate in different altitudes corresponds very well to the SCOD change rate, where the larger SCOD advancement rightly corresponds to the higher SCD increase significantly. This indicates that the SCD change in these altitudes could also be mainly related to the SCOD. The change of SCED in these altitudes further supports the indication. The SCED is slightly delayed between 900 and 1400 m, which has little influence on the SCD. The SCED advances from 1400 to 4500 m, which should theoretically lead to the shorter SCD, but the SCD is actually extended in these altitudes.

As for the high altitudes above 4500 m, the temporal change of SCD is almost zero because of the permanent snow, where the SCOD and SCED are also almost unchanged as shown in Figure 5.

5.2 | Which is more important for snow phenology in different altitudes: temperature or precipitation?

According to the vertical distribution of snow phenology and temperature/precipitation as shown in Figure 6, we can know that, as the altitude increases, the extended SCD, the advanced SCOD, and the advanced SCED coincide with the gradually increased temperature and decreased precipitation. In addition, considering the temporal change of temperature and precipitation in the sensitive period for each snow phenology measure, in most altitudes, snow phenology, including SCD, SCOD, and SCED, are significantly related to the changed temperature and/or precipitation, except for the SCD and SCOD in high altitudes, where the precipitation apparently decreases and the temperature apparently increases together with the small changes of snow phenology, which may result in the complicated correlation relationship between snow phenology and temperature/precipitation in these altitudes, as shown in Figure 8. A remaining question is to discriminate the relative importance between temperature and precipitation for snow phenology in different altitudes.

As for SCD, we could find that the temperature is more important than precipitation below 3600 m indicated by the larger correlation coefficients. Above 3600 m, the correlations between SCD and temperature/

precipitation become complicated and neither of them shows overwhelming importance than the other. Accordingly, the 3600 m is assumed as an altitude threshold to discriminate the relative importance of temperature and precipitation for SCD, because both the temperature and the precipitation changes above 3600 m become larger than those below 3600 m (Figure 9a,b), which result in the complicated correlations above 3600 m.

In terms of SCOD, the correlations to temperature are significant and apparently higher than those to precipitation below 3600 m, indicating the higher importance of temperature in these altitudes. The correlations between SCOD and temperature/precipitation also become complicated above 3600 m and neither of them indicates consistent higher importance than the other, which is also caused by the larger changes of temperature and precipitation above 3600 m (Figure 9c,d), similar to that for SCD as described above. Accordingly, the 3600 m is also assumed as the altitude threshold to discriminate the relative importance of temperature and precipitation for SCOD.

As to SCED, the correlations between SCED and temperature are significant in most cases and apparently higher than those between SCED and precipitation in almost all altitudes, indicating the more importance of temperature in different altitudes.

As a whole, we identify an altitude threshold of 3600 m to separate the relative importance of temperature and precipitation for SCD and SCOD, where the temperature shows a higher importance than precipitation below the altitude threshold, and neither temperature nor precipitation shows constant higher importance above the altitude threshold because the correlations between SCD/SCOD and temperature/precipitation become complicated. As for SCED, the temperature is consistently more important than precipitation in most altitudes. The situation of separating the relative importance of temperature and precipitation on snow phenology is somewhat different to the previous studies, for example, by Morán-Tejeda et al. (2013), Scalzitti et al. (2016), and Sospedra-Alfonso et al. (2015), where they usually find a single elevation threshold and indicate the higher importance of temperature below the threshold and the higher importance of precipitation above the threshold. The reasons for the difference could be as following: (1) The different snow cover indicator between snow phenology and snow mass; (2) The higher altitude in this study and the different climate conditions; (3) The special changes of temperature and precipitation at different altitudes in this study area, especially the larger increase of temperature and the larger decrease of precipitation in high altitude areas.

5.3 | Uncertainty of data

The daily snow cover products MOD10A1 and MYD10A1 could be affected by many factors, for example, complex terrain, cloud obscuration, and vegetation cover. Even though the cloud contamination has been removed, there are still omission errors in low altitude areas indicated by meteorological stations and commission errors in high altitude areas indicated by Landsat OLI data. MODIS snow products may underestimate the snow in forested areas (Hall and Riggs, 2007). There are several forest areas in the middle altitudes of the study area, which may bring additional errors to the calculated snow phenology besides the cloud contamination. In addition, the accuracy of the calculated snow phenology is not able to be validated in high altitude areas because of the lack of meteorological stations in these altitudes.

The accuracy of the daily surface temperature product MOD11A1 has been globally verified, and the error could achieve to be less than ± 1 k (Bosilovich, 2006; Wan, 2014). However, since the surface temperature could be affected by topography, vegetation and other factors, even though the surface temperature has been proved to be of significant correlation with air temperature (Zheng et al., 2017), the air temperature products with high-spatial and -temporal resolutions are required for improving this study. The CMFD precipitation products have strong temporal and spatial continuity and high accuracy in China (He et al., 2020), but the spatial resolution of 0.1° is still coarser compared with other products used in this study. Therefore, there is an urgently need for precipitation products with both high accuracy and high spatial resolution.

6 | CONCLUSIONS

Multi-source remote sensing data were used to explore the elevation-dependent response of snow phenology to temperature and precipitation in the north slope of Central Tianshan Mountains, China. The vertical and temporal changes of snow phenology (SCD/SCOD/SCED) and temperature/precipitation were firstly analysed, and then the correlation between snow phenology and temperature/precipitation was analysed based on the sensitive periods to reveal the elevation-dependent response as well as its vertical difference. The results show that: (1) The SCD, SCOD, and SCED tend to be extended, advanced, and slightly advanced from the hydrological year 2000 to 2018, respectively, but the temporal changes of them are various in different altitudes and contribute to the general change trends; (2) The snow phenology is significantly related to the changed temperature and/or precipitation in most altitudes, except for the SCD and SCOD in high altitudes,

where the large temporal changes of temperature and precipitation lead to the complicated correlations in these altitudes; (3) The altitude threshold of 3600 m is identified to separate the relative importance of temperature and precipitation for SCD and SCOD, where the temperature shows a higher importance than precipitation below the altitude threshold, and neither temperature nor precipitation shows constant higher importance above the altitude threshold. As for SCED, the temperature is consistently more important than precipitation in most altitudes. Since the correlation analysis method is mainly used to reveal the response of snow phenology to climate change, the physical explanations to the results are still not sufficient enough. The future work would focus on applying a snowpack physical model for explaining and projecting the changes of snow phenology in high mountains.

ACKNOWLEDGMENTS

This study is supported by the Special Subject of National Science and Technology Basic Resources Investigation (Grant No. 2017FY100503), the National Natural Science Foundation of China (Grant No. 41671344), the High-level Innovation and Entrepreneurship Talents Introduction Program of Government of Jiangsu Province of China, and the Natural Science Foundation of Jiangsu Province of China (Grant No. BK20201372).

AUTHOR CONTRIBUTIONS

Huadong Wang: Data curation; formal analysis; methodology; validation; visualization; writing - original draft; writing-review & editing. **Xueliang Zhang:** Conceptualization; data curation; formal analysis; methodology; supervision; validation; visualization; writing - original draft; writing-review & editing. **Pengfeng Xiao:** Conceptualization; supervision; writing - original draft; writing-review & editing. **Ka Zhang:** Writing - original draft; writing-review & editing. **Senyao Wu:** Writing - original draft; writing-review & editing.

ORCID

Xueliang Zhang  <https://orcid.org/0000-0001-6188-0257>

REFERENCES

- Aizen, V.B., Aizen, E.M., Melack, J.M. and Dozier, J. (1997) Climatic and hydrologic changes in the Tien Shan, Central Asia. *Journal of Climate*, 10(6), 1393–1404. [https://doi.org/10.1175/1520-0442\(1997\)010<1393:CAHCIT>2.0.CO;2](https://doi.org/10.1175/1520-0442(1997)010<1393:CAHCIT>2.0.CO;2).
- Armstrong, R.L. and Brodzik, M.J. (1995) An earth-gridded SSM/I data set for cryospheric studies and global change monitoring. *Advances in Space Research*, 16(10), 155–163. [https://doi.org/10.1016/0273-1177\(95\)00397-W](https://doi.org/10.1016/0273-1177(95)00397-W).
- Auer, I., Böhm, R., Jurkovic, A., Lipa, W., Orlik, A., Potzmann, R., et al. (2007) HISTALP: historical instrumental climatological surface time series of the greater alpine region. *International Journal of Climatology: A Journal of the Royal Meteorological Society*, 27(1), 17–46. <https://doi.org/10.1002/joc.1377>.
- Barnett, T.P., Adam, J.C. and Lettenmaier, D.P. (2005) Potential impacts of a warming climate on water availability in snow-dominated regions. *Nature*, 438(7066), 303–309. <https://doi.org/10.1038/nature04141>.
- Barry, R.G. (2002) The role of snow and ice in the global climate system: a review. *Polar Geography*, 26(3), 235–246. <https://doi.org/10.1080/789610195>.
- Beniston, M., Keller, F. and Goyette, S. (2003) Snow pack in the Swiss Alps under changing climatic conditions: an empirical approach for climate impacts studies. *Theoretical and Applied Climatology*, 74(1–2), 19–31. <https://doi.org/10.1007/s00704-002-0709-1>.
- Bi, Y., Xie, H., Huang, C. and Ke, C. (2015) Snow cover variations and controlling factors at upper Heihe River basin, northwestern China. *Remote Sensing*, 7(6), 6741–6762. <https://doi.org/10.3390/rs70606741>.
- Bosilovich, M.G. (2006) A comparison of MODIS land surface temperature with in situ observations. *Geophysical Research Letters*, 33, L20112. <https://doi.org/10.1029/2006GL027519>.
- Brown, R., Derksen, C. and Wang, L. (2010) A multi-data set analysis of variability and change in Arctic spring snow cover extent, 1967–2008. *Journal of Geophysical Research: Atmospheres*, 115, D16111. <https://doi.org/10.1029/2010JD013975>.
- Brown, R.D. and Mote, P.W. (2009) The response of northern hemisphere snow cover to a changing climate. *Journal of Climate*, 22(8), 2124–2145. <https://doi.org/10.1175/2008JCLI2665.1>.
- Brown, R.D. and Robinson, D.A. (2011) Northern hemisphere spring snow cover variability and change over 1922–2010 including an assessment of uncertainty. *The Cryosphere*, 5(1), 219–229. <https://doi.org/10.5194/tc-5-219-2011>.
- Cayan, D.R. (1996) Interannual climate variability and snowpack in the western United States. *Journal of Climate*, 9(5), 928–948. [https://doi.org/10.1175/1520-0442\(1996\)009<0928:ICVASI>2.0.CO;2](https://doi.org/10.1175/1520-0442(1996)009<0928:ICVASI>2.0.CO;2).
- Chen, X., Liang, S., Cao, Y., He, T. and Wang, D. (2015) Observed contrast changes in snow cover phenology in northern middle and high latitudes from 2001–2014. *Scientific Reports*, 5(1), 1–9. <https://doi.org/10.1038/srep16820>.
- Choi, G., Robinson, D.A. and Kang, S. (2010) Changing northern hemisphere snow seasons. *Journal of Climate*, 23(19), 5305–5310. <https://doi.org/10.1175/2010JCLI3644.1>.
- Choubin, B., Alamdarloo, E.H., Mosavi, A., Hosseini, F.S., Ahmad, S., Goodarzi, M. and Shamshirband, S. (2019) Spatio-temporal dynamics assessment of snow cover to infer snowline elevation mobility in the mountainous regions. *Cold Regions Science and Technology*, 167, 102870. <https://doi.org/10.1016/j.coldregions.2019.102870>.
- Dietz, A.J., Wohner, C. and Kuenzer, C. (2012) European snow cover characteristics between 2000 and 2011 derived from improved MODIS daily snow cover products. *Remote Sensing*, 4(8), 2432–2454. <https://doi.org/10.3390/rs4082432>.
- Ding, Y., Li, Y., Li, L., Yao, N., Hu, W., Yang, D. and Chen, C. (2018) Spatiotemporal variations of snow characteristics in Xinjiang, China over 1961–2013. *Hydrology Research*, 49(5), 1578–1593. <https://doi.org/10.2166/nh.2017.035>.
- Feng, X., Xiao, P., Zhang, X., Du, J. and Xie, S. (2018) *Remote sensing of snow in the Central Tianshan Mountains*. Beijing, China: Science Press, 533 pp (In Chinese).

- Gafurov, A. and Bárdossy, A. (2009) Cloud removal methodology from MODIS snow cover product. *Hydrology and Earth System Sciences*, 13(7), 1361–1373. <https://doi.org/10.5194/hess-13-1361-2009>.
- Gao, Y., Xie, H. and Yao, T. (2011) Developing snow cover parameters maps from MODIS, AMSR-E, and blended snow products. *Photogrammetric Engineering & Remote Sensing*, 77(4), 351–361. <https://doi.org/10.14358/PERS.77.4.351>.
- Groisman, P.Y., Karl, T.R. and Knight, R.W. (1994) Observed impact of snow cover on the heat balance and the rise of continental spring temperatures. *Science*, 263(5144), 198–200. <https://doi.org/10.1126/science.263.5144.198>.
- Hall, D.K. and Riggs, G.A. (2007) Accuracy assessment of the MODIS snow products. *Hydrological Processes: An International Journal*, 21(12), 1534–1547. <https://doi.org/10.1002/hyp.6715>.
- Hall, D.K., Riggs, G.A. and Salomonson, V.V. (1995) Development of methods for mapping global snow cover using moderate resolution imaging spectroradiometer data. *Remote Sensing of Environment*, 54(2), 127–140. [https://doi.org/10.1016/0034-4257\(95\)00137-P](https://doi.org/10.1016/0034-4257(95)00137-P).
- Hall, D.K., Riggs, G.A., Salomonson, V.V., DiGirolamo, N.E. and Bayr, K.J. (2002) MODIS snow-cover products. *Remote Sensing of Environment*, 83(1–2), 181–194. [https://doi.org/10.1016/S0034-4257\(02\)00095-0](https://doi.org/10.1016/S0034-4257(02)00095-0).
- Hamed, K.H. and Rao, A.R. (1998) A modified mann-kendall trend test for autocorrelated data. *Journal of Hydrology*, 204(1), 182–196. [https://doi.org/10.1016/S0022-1694\(97\)00125-X](https://doi.org/10.1016/S0022-1694(97)00125-X).
- Hammond, J.C., Saavedra, F.A. and Kampf, S.K. (2018) Global snow zone maps and trends in snow persistence 2001–2016. *International Journal of Climatology*, 38(12), 4369–4383. <https://doi.org/10.1002/joc.5674>.
- Harpold, A., Brooks, P., Rajagopal, S., Heidbuchel, I., Jardine, A. and Stielstra, C. (2012) Changes in snowpack accumulation and ablation in the intermountain west. *Water Resources Research*, 48, w11501. <https://doi.org/10.1029/2012WR011949>.
- He, J., Yang, K., Tang, W., Lu, H., Qin, J., Chen, Y. and Li, X. (2020) The first high-resolution meteorological forcing dataset for land process studies over China. *Scientific Data*, 7, 25. <https://doi.org/10.6084/m9.figshare.11558439>.
- Hori, M., Sugiura, K., Kobayashi, K., Aoki, T., Tanikawa, T., Kuchiki, K., Niwano, M. and Enomoto, H. (2017) A 38-year (1978–2015) northern hemisphere daily snow cover extent product derived using consistent objective criteria from satellite-borne optical sensors. *Remote Sensing of Environment*, 191, 402–418. <https://doi.org/10.1016/j.rse.2017.01.023>.
- Hu, R. (2004) *Physical geography of the Tianshan Mountains in China*. Beijing, China: China Environmental Press, 443 pp (In Chinese).
- Huang, X., Liang, T., Zhang, X. and Guo, Z. (2011) Validation of MODIS snow cover products using Landsat and ground measurements during the 2001–2005 snow seasons over northern Xinjiang, China. *International Journal of Remote Sensing*, 32(1), 133–152. <https://doi.org/10.1080/01431160903439924>.
- IPCC, Allen, M., Babiker, M., Chen, Y., & Zickfeld, K. (2018). Summary for Policymakers. In: Global warming of 1.5°C. An IPCC Special Report. Global warming of 1.5°C. An IPCC Special Report on the impacts of global warming of 1.5°C above pre-industrial levels and related global greenhouse gas emission pathways, in the context of strengthening the global response to the threat of climate change, sustainable development, and efforts to eradicate poverty.
- Kapnick, S. and Hall, A. (2012) Causes of recent changes in western north American snowpack. *Climate Dynamics*, 38(9–10), 1885–1899. <https://doi.org/10.1007/s00382-011-1089-y>.
- Ke, C.Q., Li, X.C., Xie, H., Ma, D.H., Liu, X. and Kou, C. (2016) Variability in snow cover phenology in china from 1952 to 2010. *Hydrology and Earth System Sciences*, 12(4), 4471–4506. <https://doi.org/10.5194/hess-20-755-2016>.
- Kräuchi, N., Brang, P. and Schönenberger, W. (2000) Forests of mountainous regions: gaps in knowledge and research needs. *Forest Ecology and Management*, 132(1), 73–82. [https://doi.org/10.1016/S0378-1127\(00\)00382-0](https://doi.org/10.1016/S0378-1127(00)00382-0).
- Li, C., Su, F., Yang, D., Tong, K., Meng, F. and Kan, B. (2018) Spatiotemporal variation of snow cover over the Tibetan Plateau based on MODIS snow product, 2001–2014. *International Journal of Climatology*, 38(2), 708–728. <https://doi.org/10.1002/joc.5204>.
- Liang, T.G., Huang, X.D., Wu, C.X., Liu, X.Y., Li, W.L., Guo, Z.G. and Ren, J.Z. (2008) An application of MODIS data to snow cover monitoring in a pastoral area: a case study in northern Xinjiang, China. *Remote Sensing of Environment*, 112(4), 1514–1526. <https://doi.org/10.1016/j.rse.2007.06.001>.
- Ma, N., Yu, K., Zhang, Y., Zhai, J. and Zhang, H. (2020) Ground observed climatology and trend in snow cover phenology across China with consideration of snow-free breaks. *Climate Dynamics*, 55, 2887. <https://doi.org/10.1007/s00382-020-05422-z>.
- McKay, G. and Thompson, H.A. (1968) Snowcover in the prairie provinces of Canada. *Transactions of the ASAE*, 11(6), 812–815. <https://doi.org/10.13031/2013.39529>.
- Morán-Tejeda, E., López-Moreno, J.I. and Beniston, M. (2013) The changing roles of temperature and precipitation on snowpack variability in Switzerland as a function of altitude. *Geophysical Research Letters*, 40(10), 2131–2136. <https://doi.org/10.1002/grl.50463>.
- Najafi, M.R., Zwiers, F.W. and Gillett, N.P. (2016) Attribution of the spring snow cover extent decline in the northern hemisphere, Eurasia and North America to anthropogenic influence. *Climatic Change*, 136(3–4), 571–586. <https://doi.org/10.1007/s10584-016-1632-2>.
- Notarnicola, C. (2020) Hotspots of snow cover changes in global mountain regions over 2000–2018. *Remote Sensing of Environment*, 243, 111781. <https://doi.org/10.1016/j.rse.2020.111781>.
- Parajka, J. and Blöschl, G. (2008) Spatio-temporal combination of MODIS images–potential for snow cover mapping. *Water Resources Research*, 44, W03406. <https://doi.org/10.1029/2007WR006204>.
- Peng, S., Piao, S., Ciais, P., Friedlingstein, P., Zhou, L. and Wang, T. (2013) Change in snow phenology and its potential feedback to temperature in the northern hemisphere over the last three decades. *Environmental Research Letters*, 8(1), 014008. <https://doi.org/10.1088/1748-9326/8/1/014008>.
- Pu, Z., Xu, L. and Salomonson, V.V. (2007) MODIS/Terra observed seasonal variations of snow cover over the Tibetan plateau. *Geophysical Research Letters*, 34, L06706. <https://doi.org/10.1029/2007GL029262>.
- Räisänen, J. (2008) Warmer climate: less or more snow? *Climate Dynamics*, 30(2–3), 307–319. <https://doi.org/10.1007/s00382-007-0289-y>.
- Rango, A. (1997) The response of areal snow cover to climate change in a snowmelt–runoff model. *Annals of Glaciology*, 25, 232–236. <https://doi.org/10.3189/S0260305500014099>.

- Redpath, T.A.N., Sirguey, P. and Cullen, N.J. (2019) Characterising spatio-temporal variability in seasonal snow cover at a regional scale from modis data: the clutha catchment, New Zealand. *Hydrology and Earth System Sciences*, 23(8), 3189–3217. <https://doi.org/10.5194/hess-23-3189-2019>.
- Scalzitti, J., Strong, C. and Kochanski, A. (2016) Climate change impact on the roles of temperature and precipitation in western US snowpack variability. *Geophysical Research Letters*, 43(10), 5361–5369. <https://doi.org/10.1002/2016GL068798>.
- Scherrer, S.C., Appenzeller, C. and Laternser, M. (2004) Trends in Swiss alpine snow days: the role of local-and large-scale climate variability. *Geophysical Research Letters*, 31, L13215. <https://doi.org/10.1029/2004GL020255>.
- Sinha, T. and Cherkauer, K.A. (2008) Time series analysis of soil freeze and thaw processes in Indiana. *Journal of Hydrometeorology*, 9(5), 936–950. <https://doi.org/10.1175/2008JHM934.1>.
- Sospedra-Alfonso, R., Melton, J.R. and Merryfield, W.J. (2015) Effects of temperature and precipitation on snowpack variability in the central Rocky Mountains as a function of elevation. *Geophysical Research Letters*, 42(11), 4429–4438. <https://doi.org/10.1002/2015GL063898>.
- Sun, Y., Zhang, T., Liu, Y., Zhao, W. and Huang, X. (2020) Assessing snow phenology over the large part of Eurasia using satellite observations from 2000 to 2016. *Remote Sensing*, 12(12), 2060. <https://doi.org/10.3390/rs12122060>.
- Tang, Z., Wang, X., Wang, J., Wang, X., Li, H. and Jiang, Z. (2017) Spatiotemporal variation of snow cover in Tianshan Mountains, Central Asia, based on cloud-free MODIS fractional snow cover product, 2001–2015. *Remote Sensing*, 9(10), 1045. <https://doi.org/10.3390/rs9101045>.
- Tong, J., Déry, S.J. and Jackson, P.L. (2009) Topographic control of snow distribution in an alpine watershed of western Canada inferred from spatially-filtered MODIS snow products. *Hydrology and Earth System Sciences*, 13(3), 319–326. <https://doi.org/10.5194/hess-13-319-2009>.
- Viviroli, D., Archer, D.R., Buytaert, W., Fowler, H.J., Greenwood, G.B., Hamlet, A.F., et al. (2011) Climate change and mountain water resources: overview and recommendations for research, management and policy. *Hydrology and Earth System Sciences*, 15(2), 471–504. <https://doi.org/10.5194/hess-15-471-2011>.
- Wan, Z. (2014) New refinements and validation of the collection-6 MODIS land-surface temperature/emissivity product. *Remote Sensing of Environment*, 140, 36–45. <https://doi.org/10.1016/j.rse.2013.08.027>.
- Wang, W., Liang, T., Huang, X., Feng, Q., Xie, H., Liu, X., Chen, M. and Wang, X. (2013) Early warning of snow-caused disasters in pastoral areas on the Tibetan plateau. *Natural Hazards & Earth System Sciences*, 13(6), 1411–1425. <https://doi.org/10.5194/nhess-13-1411-2013>.
- Wang, X. and Xie, H. (2009) New methods for studying the spatio-temporal variation of snow cover based on combination products of MODIS Terra and Aqua. *Journal of Hydrology*, 371(1–4), 192–200. <https://doi.org/10.1016/j.jhydrol.2009.03.028>.
- Wang, Z., Wu, R. and Huang, G. (2018) Low-frequency snow changes over the Tibetan plateau. *International Journal of Climatology*, 38(2), 949–963. <https://doi.org/10.1002/joc.5221>.
- Woo, M.K. and Thorne, R. (2006) Snowmelt contribution to discharge from a large mountainous catchment in subarctic Canada. *Hydrological Processes: An International Journal*, 20(10), 2129–2139. <https://doi.org/10.1002/hyp.6205>.
- Wu, S., Zhang, X., Du, J., Zhou, X., Tuo, Y., Li, R. and Duan, Z. (2019) The vertical influence of temperature and precipitation on snow cover variability in the central Tianshan Mountains, Northwest China. *Hydrological Processes*, 33(12), 1686–1697. <https://doi.org/10.1002/hyp.13431>.
- Xie, H., Wang, X. and Liang, T. (2009) Development and assessment of combined Terra and Aqua snow cover products in Colorado plateau, USA and northern Xinjiang, China. *Journal of Applied Remote Sensing*, 3(1), 033559. <https://doi.org/10.1117/1.3265996>.
- Yang, J., Jiang, L., Ménard, C.B., Luojus, K., Lemmetyinen, J. and Pulliainen, J. (2015) Evaluation of snow products over the tibetan plateau. *Hydrological Processes*, 29(15), 3247–3260. <https://doi.org/10.1002/hyp.10427>.
- Ye, B., Yang, D., Jiao, K., Han, T., Jin, Z., Yang, H. and Li, Z. (2005) The Urumqi River source glacier No. 1, Tianshan, China: changes over the past 45years. *Geophysical Research Letters*, 32, L21504. <https://doi.org/10.1029/2005GL024178>.
- Ye, H. (2001) Increases in snow season length due to earlier first snow and later last snow dates over north central and Northwest Asia during 1937–94. *Geophysical Research Letters*, 28(3), 551–554. <https://doi.org/10.1029/2000GL012036>.
- You, Q., Kang, S., Ren, G., Fraedrich, K., Pepin, N., Yan, Y. and Ma, L. (2011) Observed changes in snow depth and number of snow days in the eastern and central Tibetan plateau. *Climate Research*, 46(2), 171–183. <https://doi.org/10.3354/cr00985>.
- Zheng, W., Du, J., Zhou, X., Song, M., Bian, G., Xie, S. and Feng, X. (2017) Vertical distribution of snow cover and its relation to temperature over the Manasi River basin of Tianshan Mountains, Northwest China. *Journal of Geographical Sciences*, 27(4), 403–419. <https://doi.org/10.1007/s11442-017-1384>.
- Zhu, W., Shangguan, D., Guo, W. and Xu, J. (2014) Glaciers in some representative basins in the middle of the Tianshan Mountain: change and response to climate change. *Journal of Glaciology and Geocryology*, 36(06), 1376–1384 (In Chinese).

How to cite this article: Wang, H., Zhang, X., Xiao, P., Zhang, K., & Wu, S. (2022). Elevation-dependent response of snow phenology to climate change from a remote sensing perspective: A case survey in the central Tianshan mountains from 2000 to 2019. *International Journal of Climatology*, 42(3), 1706–1722. <https://doi.org/10.1002/joc.7330>